Turkish Journal of Chemistry

http://journals.tubitak.gov.tr/chem/

Research Article

Turk J Chem
(2020) 44: 125 – 141

doi:10.3906/kim-1906-23

Highly improved electrocatalytic oxidation of dimethylamine borane on silver nanoparticles modified polymer composite electrode

Çağrı Ceylan KOÇAK[1], **Süleyman KOÇAK**[2], **Şükriye KARABİBEROĞLU**[3], **Zekerya DURSUN**[3,*]

[1]Bergama Vocational School, Dokuz Eylül University, İzmir, Turkey
[2]Department of Chemistry, Faculty of Science and Letters, Manisa Celal Bayar University, Manisa, Turkey
[3]Department of Chemistry, Faculty of Science, Ege University, İzmir, Turkey

Received: 20.06.2019 • **Accepted/Published Online:** 04.11.2019 • **Final Version:** 11.02.2020

Abstract: Dimethylamine borane (DMAB) is a promising fuel alternative for fuel cell applications. In this work cyclic voltammetric behavior of DMAB was investigated on the polymerized aminophenol film decorated with Ag nanoparticles in alkaline media. The polymer film was formed on the glassy carbon electrode by electrochemical technique and then, the surface was modified with Ag nanoparticles. The surface of the modified electrode was identified by scanning electron microscopy, transmission electron microscopy, X-ray photoelectron spectroscopy, and electrochemical impedance spectroscopy techniques. The developed electrode has displayed high electrocatalytic activity for DMAB oxidation in alkaline media depending on the supporting electrolyte concentration. Experimental parameters such as cycle number used in electropolymerization of p-aminophenol, deposition of Ag nanoparticles and supporting electrolyte were optimized.

Key words: Dimethylamine borane, silver nanoparticles, poly(aminophenol), fuel cell, scanning electron microscopy

1. Introduction

Fossil-based energy resources give rise to environmental problems that led researchers to find alternative renewable energy sources. In recent years, fuel cell developments have received great attention due to their low emissions to environment and high efficiencies. Fuel cells convert chemical energy stored in fuels to electrical energy and therefore require a constant source of fuel to sustain the chemical reaction [1–3].

Dimethylamine borane (DMAB) has amine odor and a chemical formula of $(CH_3)_2NH{:}BH_3$ [4]. DMAB is used in wide range of applications as a reductant [5–7] and is also used as a fuel in fuel cell applications [8,9]. In recent years, studies on the use and research of boron-derived fuels have become widespread all over the world [10–12]. DMAB is a boron derivative fuel and it is important to examine its possible behavior as an alternative energy source. For this purpose, some researchers have studied the oxidation reaction of DMAB [9,13,14]. Generally, from the reaction of DMAB in the alkaline solution, the hydroxytrihydroborate intermediate anion occurs [9,14,15]. Two mechanisms have been proposed for DMAB oxidation on the different gold electrode. Plana and Dryfe [9] and Plana et al. [14] reported that the hydroxytrihydroborate anion is either converted to water with 6 electron yields, or a lower-efficiency oxidation process may produce molecular hydrogen with 3

*Correspondence: zekerya.dursun@ege.edu.tr

electron yields. The general mechanism of DMAB has been proposed as an integer between 3 and 6 [9,14]. The anode reaction of the direct DMAB fuel cell is the direct oxidation of DMAB in alkaline medium as follows:

$$(CH_3)_2NH\ BH_{3(aq)} + OH^-_{(aq)} \rightarrow BH_3OH^-_{(aq)} + (CH_3)_2NH_{(aq)} \quad (1)$$

The hydroxytrihydroborate anion generally follows the possible two ways: First one is six-electron pathway (high efficiency) [13,16,17]:

$$BH_3OH^-_{(aq)} + 6OH^-_{(aq)} \rightarrow B(OH)^-_{4\ (aq)} + 3H_2O_{(l)} + 6e^- \quad (2)$$

The second pathway yields three electrons and molecular hydrogen (lower efficiency):

$$BH_3OH^-_{(aq)} + 3OH^-_{(aq)} \rightarrow B(OH)^-_{4\ (aq)} + (3/2)\ H_{2(g)} + 3e^- \quad (3)$$

The hydrolysis of DMAB resulted in the formation of hydrogen gas as the anode fuel (Eq. (3)). On the other hand, direct DMAB oxidation provides an improved cell voltage compared with oxidizing molecular hydrogen. Competing chemical hydrolysis of DMAB with evolution of hydrogen, given by Eq. 3, is expected to be minimal at pH values in excess of 12.

To date, there have been only a few studies which attempt to explain the mechanism of DMAB direct electrooxidation. In one of these studies, the oxidation of DMAB on polycrystalline gold electrodes was investigated by Plana and Dryfe [9]. Two sequential oxidation processes took place on gold surface. Three e^- are removed from DMAB, so H_2 is not oxidized at low potentials. A six-electron was extracted from molecule at high potential. Another study about direct electrooxidation of DMAB was conducted by Nagle and Rohan [13]. It explained that an overall coulomb number of six has been determined from the data acquired using the diffusion coefficient determined and the number of electrons in the oxidation reaction depends on the OH–DMAB ratio and the hydrogen content becomes increasingly important as this ratio decreases. The direct electrooxidation of DMAB was also investigated with Au and Pt bulk surface by Finkelstein et al. [18]. This study assumed that DMAB completely dissociates as in Eq. (1). Another finding is that DMAB oxidation has two distinct oxidation processes taking place at low potential region and high potential region.

Metal nanoparticles have attracted great attention for their unique physical and chemical properties owing to their high surface area to volume ratio that differs from their bulk forms [19,20]. Wide range of techniques such as microemulsion [21], sol-gel [22], thermal reduction [23], metal vapor [24], and chemical reduction [25,26] have been used for their synthesis. Electrochemical synthesis, on the other hand, has drawn particular attention as an inexpensive and rapid technique with an advantage of controlling over the particle size by changing the conditions. Metal nanoparticles are usually deposited on a support for stability such as conducting polymers [27]. Pt, Au, Pd, etc. are widely studied metal nanoparticles in various kinds of applications [28–31]. Although the efficiency obtained in the presence of these metals is high, the cost considerably increases. Therefore, there is a need for cheaper and highly effective alternative catalytic surfaces. Ag has an important place among other alternative metals due to its good catalytic activity, biocompatibility, ability for accelerating the electron transfer and electro-conductibility [32]. Different silver forms offered good catalytic activity for such analytes [33–35]. In addition, the price is quite low compared to precious metals, which is an important parameter for applications [36]. In this regard, Ag nanoparticle modified surface is designed as a candidate for an active surface to energy application.

Polymers are promising materials for the preparation of nanocomposites. Conducting polymers have attracted significant attention because of their chemical, mechanical, optical, and electrical properties [37–39]. Due to their unique properties, a variety of conducting polymers are used in analytical applications [40] as well as catalytic surfaces in fuel cells [41–44]. Recently, some reports have been published by our research group about application of polymer modified electrodes on neurotransmitter detection [45], oxygen reduction [46], ammonia borane investigation [47], and antimony detection [48]. In each substrate polymeric structure has provided long-term stability for metal nanoparticles. Compared to all other polymers, electroactive aminophenol polymer (PAP) is remarkable in its various properties. In different environments, it has the ability to form highly conductive film on different surfaces [49–51]. Active functional groups in its structure both facilitate the polymerization on the electrode surface and form a selective surface for many analytes [46,52–54]. PAP-modified surfaces maintain their conducting properties for a long time as compared to many conductive polymers [55]. Chemically stable homogeneous PAP films with controlled thickness can be achieved with electrochemical modification [56]. When all these mentioned features are evaluated, PAP stands out as a preferred modifier.

Present work describes the fabrication of oxidized Poly (p-aminophenol) film modified electrode decorated with Ag nanoparticles (AgNPs) for the investigation of DMAB oxidation in alkaline solutions. The electrode surface was characterized with scanning electron microscopy (SEM), transmission electron microscopy (TEM) energy-dispersive X-ray spectroscopy (EDX), X-Ray photoelectron spectroscopy (XPS) and electrochemical impedance spectroscopy (EIS). Experimental parameters both in electropolymerization and DMAB oxidation were optimized and the results of electrocatalytic oxidation of DMAB at the AgNPs-modified oxidized polymer film electrode were compared with those obtained with bare GCE and polymer film electrode.

2. Materials and methods

2.1. Reagents and instrumentation

The monomer, p-aminophenol, was obtained from Fluka and the fuel, DMAB, was purchased from Alfa Aesar. NaOH reagent was obtained from Raidel De Haen. Sodium dodecylsulfate (SDS) and $HClO_4$ reagents were of analytical-reagent grade and supplied from Sigma. $AgNO_3$ was purchased from Carlo Erba. All the solutions were prepared using ultrapure water. All electrochemical experiments were carried out under nitrogen gas.

Autolab 302N was used as voltammetric analyzer for measurements. Three electrode systems consisting of a working electrode, a platinum wire counter electrode, and an Ag/AgCl (sat. KCl) reference electrode were employed in measurements. Glassy carbon electrode (0.0707 cm^2) was obtained from BASi. The surface characterization was examined by using Thermo K-Alpha-Monochromated high-performance XPS spectrometer (XPS), JEOL JEM-ARM200F transmission electron microscopy (TEM), and Philips XL30 SFEG scanning electron microscopy (SEM).

2.2. Electrochemical measurements

Cyclic voltammetry (CV) and chronoamperometry were used for electrochemical measurements. CVs were carried out between –1300 mV and 0 mV with 50 mV s^{-1} scan rate in 2.0 M NaOH containing DMAB. Chronoamperometric responses were recorded in a 2.0 M NaOH solution at peak potentials of Ag wire and AgNPs/PAP/GCE towards DMAB with 0.5 s time interval.

2.3. Preparation of working electrodes

Before modification, the GCE was polished with alumina slurry (0.05–3 µm) and rinsed with pure water. For removing any residues, the electrode was subjected to ultrasonication in ethanol (1:1, v/v) and ultrapure water. The GCE was then immersed in a 5 mM SDS and p-aminophenol containing 0.5 M $HClO_4$ solution and electrochemical deposition of poly(p-aminophenol) on GCE was performed by cyclic voltammetry technique as given elsewhere [57]. Polymerized film was obtained by consecutive 35 potential cycles with 100 mV s^{-1} scan rate from –0.5 V to 2 V. The resulting electrode was abbreviated as PAP/GCE.

AgNPs were deposited on the PAP/GCE surface using electrochemical reduction of silver ions from 2 mM $AgNO_3$ on the PAP/GCE in 0.1 M HNO_3 solution. It was performed by ten repetitive cyclic voltammograms in the potential range of 0.3 V and –0.9 V.

3. Results and discussion

3.1. Surface characterizations of electrodes

The surface morphologies of the electrodes were characterized by XPS, SEM, TEM, and EIS. Figures 1A–1C show the SEM images of AgNPs/PAP/GCE with different magnifications which exhibit the good surface coverage with polymer film and AgNPs. Spherical AgNPs are distributed homogeneously on the polymerized electrode surface. The presence of Ag element on the PAP/GCE surface was analyzed by Energy Dispersive X-ray (EDX) spectroscopy (Figure 1D). The weight gain of the PAP/GCE because of the Ag loading was found nearly 8.7%. The overall data has confirmed that uniform coverage of Ag on the PAP/GCE can be achieved with cyclic voltammetry. The size distribution of the Ag nanoparticles obtained from SEM analysis was shown in Figure 1E. The particle size ranges from 2 to 160 nm and the average particle size was found approximately 100 nm. Moreover, TEM image of AgNP-modified PAP surface (Figure 1F) exhibited small spherical and flower-like structures related to the AgNPs. Comparison of SEM and TEM images point out that the Ag metal particles' diameters were not identical because of the application of different preparation procedures for SEM and TEM samples. For the SEM measurements, the electrochemically prepared composite surface was scanned by the SEM system; thus, the AgNPs/PAP/GCE surface was maintained. In addition, in TEM measurements, the electrochemically prepared polymer and Ag metal particles' content were transferred to ethanol solvent by scraped from the electrode surface with a sharp knife and then TEM grids. The Ag metal particles should be liberated to smaller particles. Accordingly, number of the Ag metal particles in the SEM image was higher than that in the TEM image.

XPS technique provides important information about bonding characteristics of the film and oxidation states of Ag nanoparticles. Figure 2A shows the wide spectrum of poly(p-aminophenol) film. It is evident that Ag3d, C1s, O1s, and N1s signals are present in polymer structure. For each curve-fitted region, the component peaks are numbered and chemical state assignment was identified based on literature data [58–60]. The curve fitting of the C1s peaks for PAP/GCE has been done by assuming two components at 284.7 and 286.2 respectively (Figure 2B). These values could correspond to C-N and C-O groups, on the basis of the PAP chemical formula. The fitted O1s spectra of the PAP modified GC electrodes were shown in Figure 2C. Two oxygen species were observed with the PAP/GCE (Figure 2B-1) at BE 531.7 and 533.3 eV. The lower BE signal (531.7 eV) could be assigned to –C-O bond. The BE at 533.3 eV could be due to typical of phenolic/ether oxygen. Figure 2D shows the fitted N1s spectra indicating one component centered at 400.2 eV, a binding energy typical of C-N groups in the polymeric chain. Figure 2E shows the XPS spectra of AgNPs/PAP/GCE

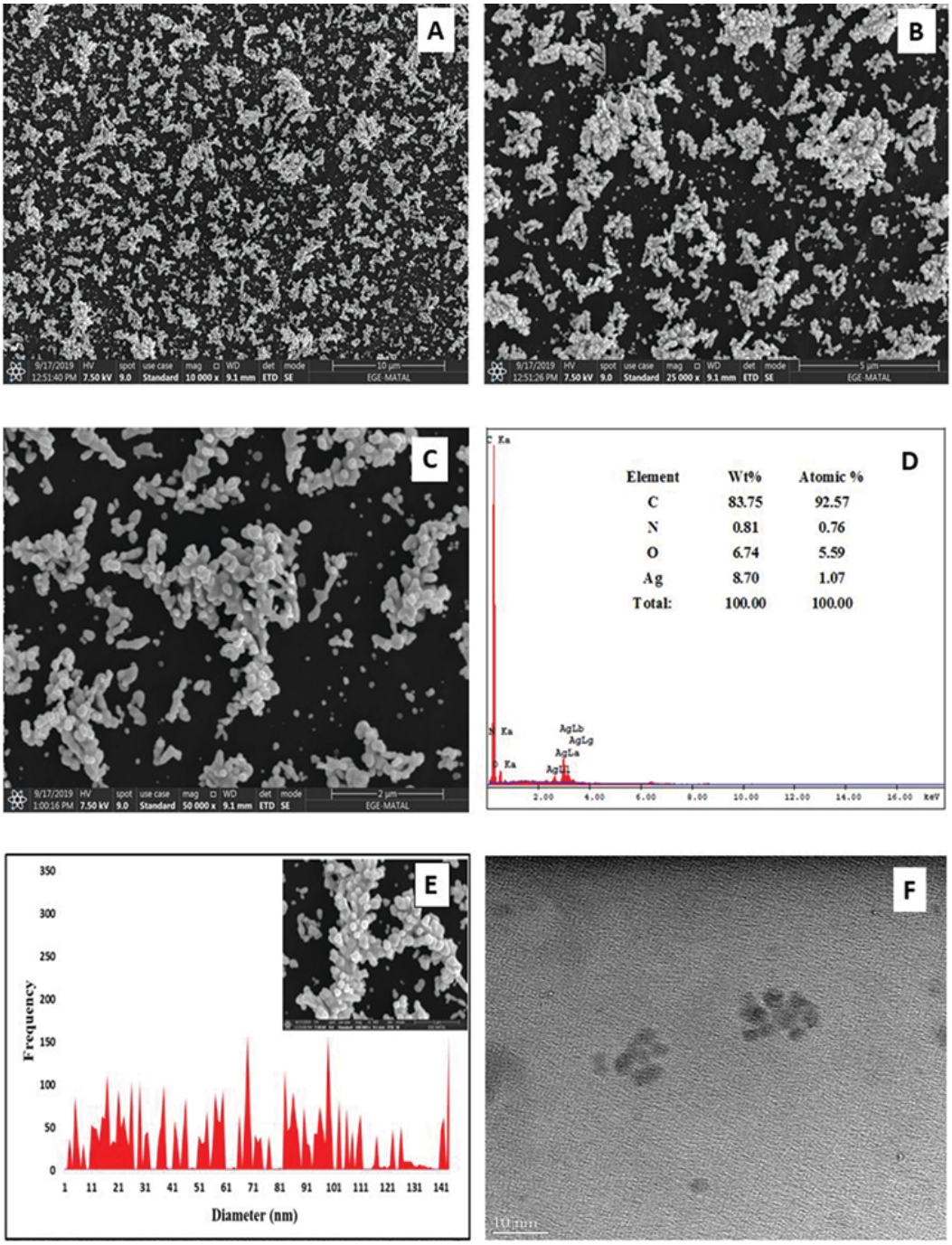

Figure 1. SEM images with different magnifications (A-C), EDX results (D), size distribution (shaded bars) of AgNPs on the PAP surface and TEM image (F) of AgNPs/PAP/GCE.

in Ag3d region. Ag doublets of $Ag3d_{5/2}$ and $Ag3d_{3/2}$ were observed at binding energies of 368.39 and 374.08 eV, respectively. The results verified that Ag species inside the aminophenol polymer film were chiefly dispersed as metallic Ag [61,62]. Moreover, the amount of Ag was found as 34.4 µg cm^{-2} according to the experimental results.

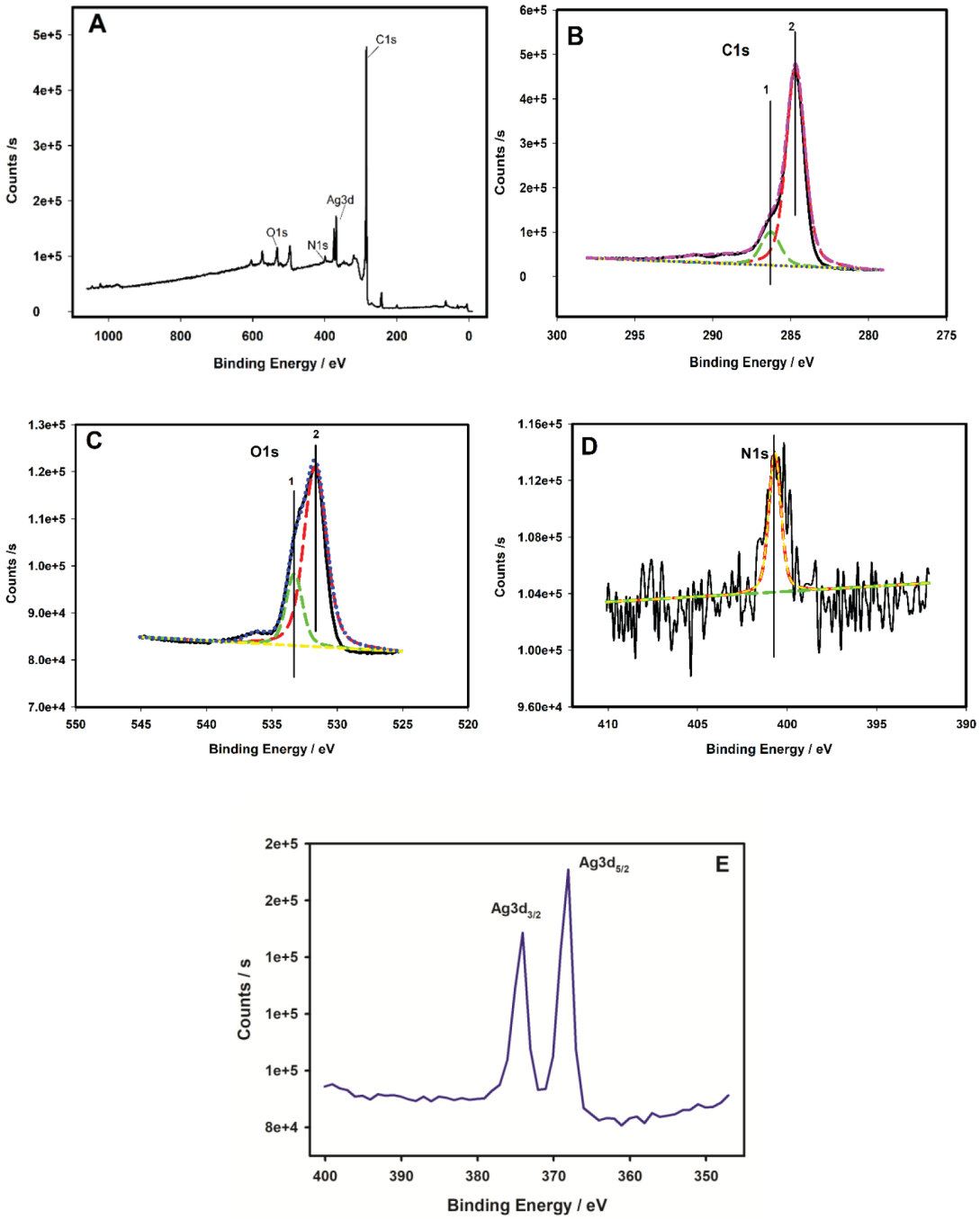

Figure 2. (A) XPS survey spectrum of AgNPs/PAP/GCE; core level spectra of (B) C1s, (C) O1s, (D) N1s, and (E) Ag3d.

EIS was performed in 5 mM DMAB containing 2 M NaOH solution in the frequency range of 50,000 to 0.05 Hz. The normalized Nyquist plots were represented in Figure 3A and results were fitted with (R(RC)) equivalent circuit. The highest electron transfer resistance was obtained at bare GCE. This value was decreased with polymer coating on the surface and reached its smallest value with subsequent Ag modification. As seen from the results, lower solution resistance and DMAB oxidation impedance indicate that DMAB is more easily

oxidized on the AgNPs/PAP/GCE surface as compared to the GCE and PAP/GCE. In addition, Bode plots were shown in Figure 3B. They reveal the signs of redox activity both in the modulus of the impedance and the phase angle. The double sigmoid is visible at low frequency in modulus impedance. According to the phase angle, capacitive behavior is observed over a narrow frequency range and where a second capacitive contribution is seen between 1 and 10 Hz. This behavior is indicative of residual, albeit hindered, redox activity at the electrode surface. The impedance value was increased with the modification of PAP and AgNPs on the GCE surface. This behavior was found related with the faster electron transfer rate. At the intermediate frequencies the phase angle value remains almost the same for all electrodes. The same phase angle indicates that all electrodes have the same capacitive properties.

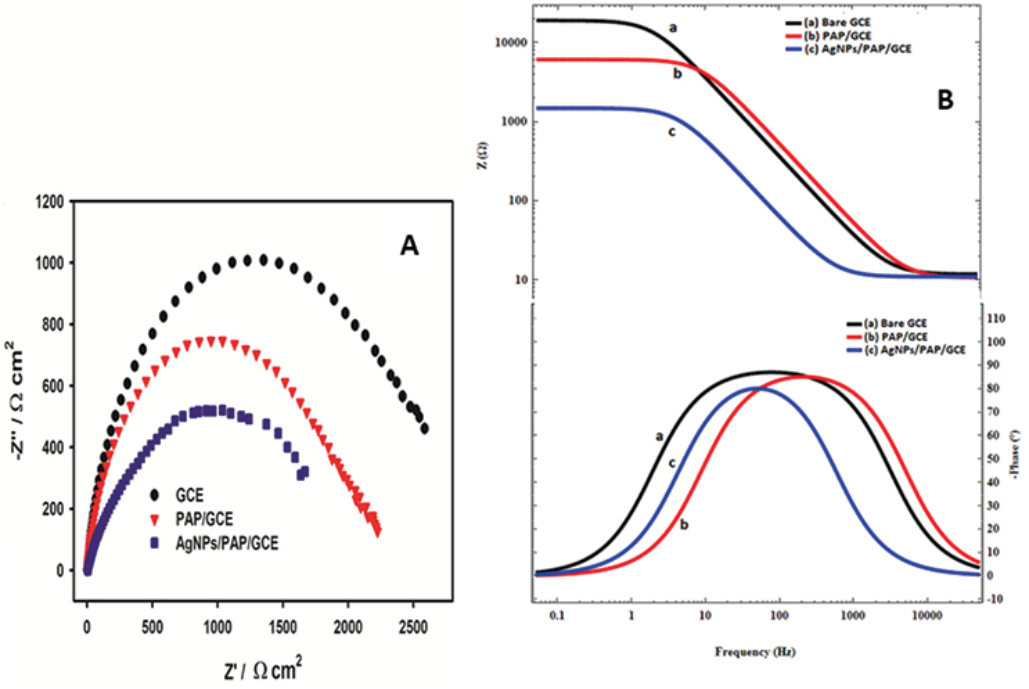

Figure 3. A) Normalized Nyquist plots B) Bode plots of bare and modified electrodes in 2.0 M NaOH containing 5.0 mM DMAB (frequencies: from 50 000 to 0.05 Hz).

3.2. Electroactive surface area

In this study, the electroactive surface area (ESA) was via CV by employing the increasing scan rates on AgNPs/PAP/GCE in 0.1 M KCl containing 0.5 mM $K_3Fe(CN)_6/K_4Fe(CN)_6$ couple. $K_3Fe(CN)_6/K_4Fe(CN)_6$ involves one electron per molecule redox reaction [63]. Based on the obtained results, square root of scan rate versus peak current plot was drawn. ESA of the bare and modified electrodes were calculated with the help of Randles–Sevcik equation (4):

$$i_p = \left(2.69\ 10^5\right) n^{3/2} A\, C\, D^{1/2}\, v^{1/2} \tag{4}$$

D (diffusion coefficient) was taken as 6.70×10^{-6} cm^2 s^{-1}, $K_3Fe(CN)_6/K_4Fe(CN)_6$ concentration (C) was added to the equation, n is the transferred electron number in the redox system was taken as 1, active area (A) is the only unknown component in the equation that calculated from the result of the equation [64]. ESA of

the electrodes were found as 0.056 cm^2, 0.290 cm^2, and 0.574 cm^2 for GCE, PAP/GCE and AgNPs/PAP/GCE, respectively. Presence of PAP and AgNPs lead to an increase on the electroactive area of GCE. The larger electroactive surface area confirms the higher activity toward DMAB oxidation.

3.3. Electrocatalytic oxidation of DMAB

The performance of the electrodes towards DMAB oxidation was tested by cyclic voltammetry in alkaline media. Figure 4 demonstrates the cyclic voltammograms obtained with the bare, PAP/GCE, and AgNPs/PAP/GCE electrodes in the presence (Figure 4) and absence (Figure 4-inset) of 1 mM DMAB solution in 2 M NaOH. The AgNPs/PAP/GCE has displayed an excellent catalytic activity towards DMAB oxidation in comparison to the bare electrode and PAP/GCE. A well-defined irreversible oxidation peak was observed at –916 mV with 0.36 mA cm^{-2} current value at the AgNPs/PAP/GCE, while there is no response obtained at bare and PAP/GCE for DMAB oxidation.

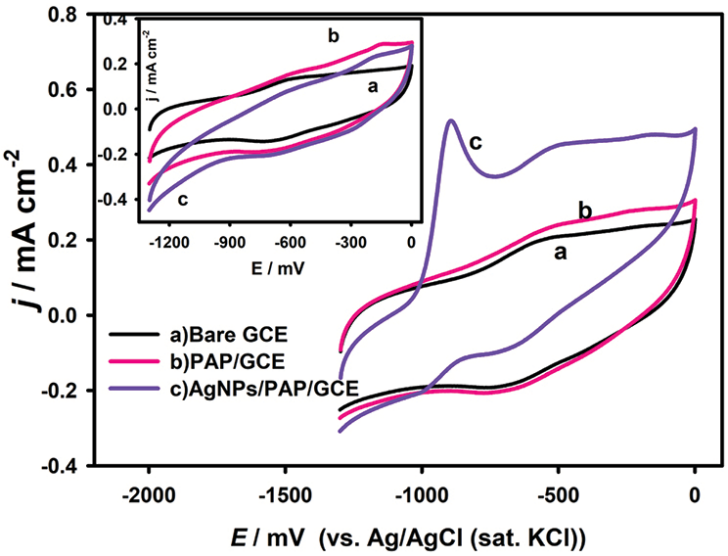

Figure 4. CVs of bare GCE, PAP/GCE and AgNPs/PAP/GCE in 2.0 M NaOH containing 1.0 mM DMAB. Inset: Background voltammograms.

In fuel cell studies, alkaline media is preferred for operational purposes. The effect of NaOH concentrations on the DMAB oxidation was investigated in the concentration range of 0.05 to 4.00 M (Figure 5A). The peak currents related with the DMAB oxidation have shown an increase up to 2 M and then decreased for more concentrated solutions of NaOH. The change in the peak current was accompanied by the shift in the peak potential by increasing NaOH concentration. It has been known that DMAB is relatively stable at high pH values [9]. Therefore, 2 M NaOH medium was selected as the optimum supporting electrolyte since it provides high peak current and a satisfactory shift in the peak potential. Electrochemical polymerization offers an advantage of tuning the polymeric film thickness and nanoparticle size/distribution which are important in terms of catalytic activity. The surface coverages of PAP/GC electrodes were adjusted by changing the cycle numbers used in polymerization from 30 to 60 in the studied potential range. Figure 5B demonstrates the effect of polymerization cycle number on the oxidation peak of 1 mM DMAB in 2 M NaOH. As can be seen clearly in Figure 5B, the peak current obtained for DMAB has given a plateau between 35 to 50 cycles while the desirable

shift in peak potential was observed at 35 cycles. Therefore, the potential was cycled from –0.5 to 2 V for 35 consecutive scans with a rate of 100 mV s^{-1} in further modification studies.

Another parameter to be optimized is the cycle number of Ag deposition which is used for nanoparticle formation. The cycle number varied from 5 to 20 and resulting peak characteristics were plotted in Figure 5C. DMAB oxidation peak current reached its maximum value with the satisfying potential value with 10 cycles of Ag deposition on PAP/GCE.

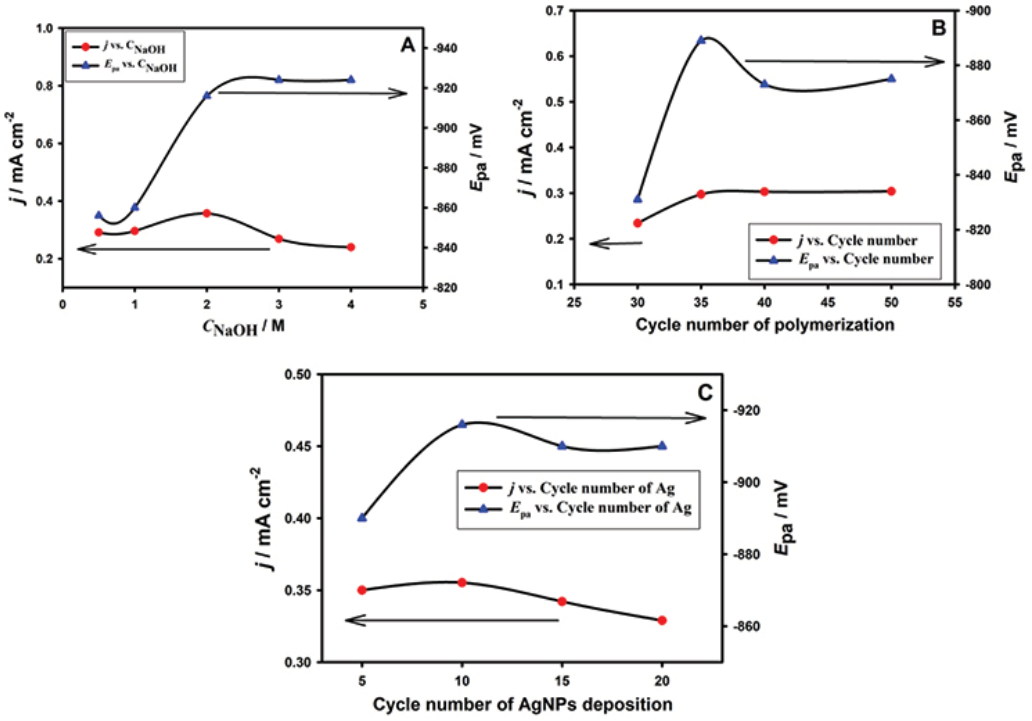

Figure 5. Anodik peak potential and current values of DMAB vs. A) NaOH concentration, B) Cycle number of PAP polymerization, and D) Cycle number of Ag deposition (AgNPs/PAP/GCE in 2.0 M NaOH containing 1 mM DMAB with 50 mV s^{-1}).

Cyclic voltammetric response of AgNPs/PAP/GCE in 1 mM DMAB containing 2 M NaOH with various scan rates were shown in Figure 6A. The peak current of DMAB was directly proportional to the square root of scan rate in the range of 3–1000 mV s^{-1}. These data show that the electrode reaction was controlled by diffusion of DMAB to electrode surface (Figure 6B). The plot of peak potential vs. logarithm of scan rate was also shown in Figure 6C. The logarithm of the scan rate has a linear dependence with peak potential; therefore, the results showed that an irreversible electrode reaction occured on the AgNPs/PAP/GCE.

The voltammetric response and corresponding calibration plot of peak currents vs. concentrations are shown in Figure 7. The curves b–e corresponds to the DMAB concentration of 1.0, 3.0, 5.0, and 8.0 mM, respectively where curve a displays the background response of electrode. The oxidation peak currents increase linearly from 0.36 to 2.33 mA cm^{-2} with a correlation of 0.9975 by changing DMAB concentration in a range of 1–8 mM. The overall data indicates the efficiency of AgNPs/PAP/GCE electrode for DMAB oxidation in alkaline media.

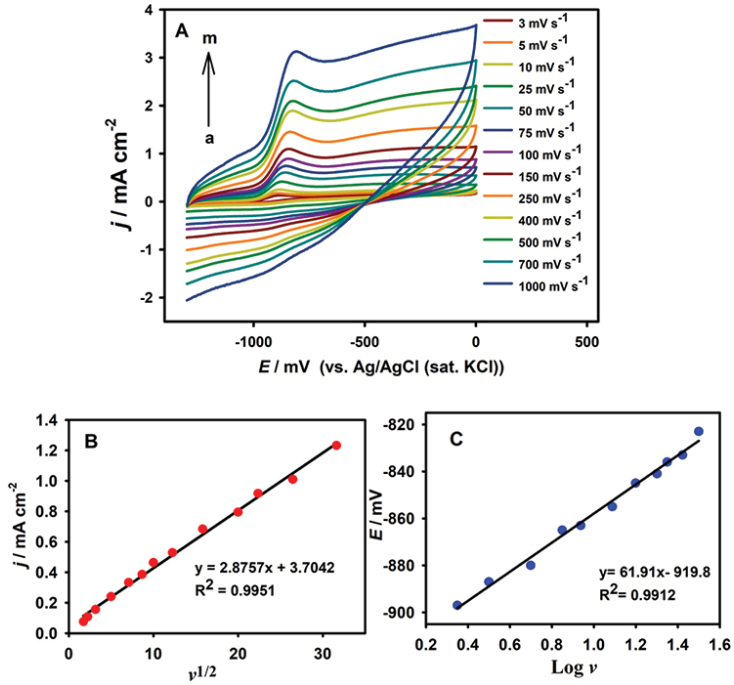

Figure 6. A) CVs of 1.0 mM DMAB oxidation in 2.0 M NaOH at increasing scan rates. a-m: 3–1000 mV s^{-1} on AgNPs/PAP/GCE. Plots of the B) Electrocatalytic current of AgNPs/PAP/GCE vs. the square root of scan rate ($v^{1/2}$), and C) Oxidation potential vs. Log v.

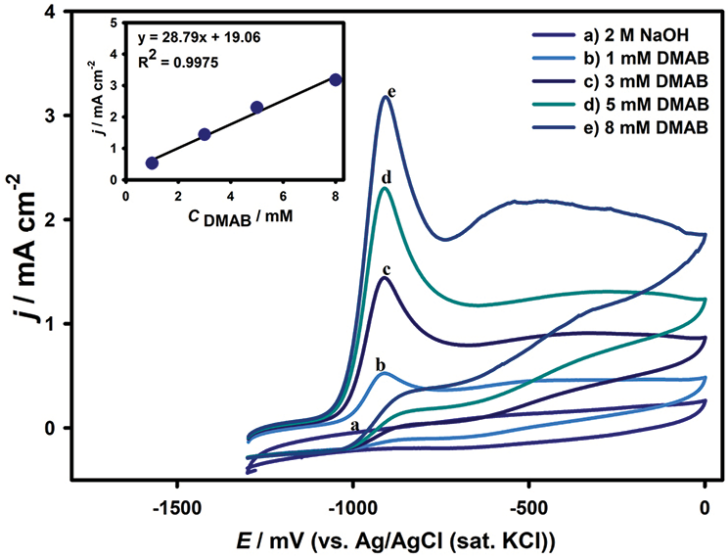

Figure 7. Cyclic voltammograms of a) Background response in 2.0 M NaOH, b) 1.0 mM, c) 3.0 mM, d) 5.0 mM, and e) 8.0 mM DMAB oxidation at AgNPs/PAP/GCE. Inset: plot for the peak current of AgNPs/PAP/GCE versus the concentration of DMAB.

3.4. Rotating disk studies

The rotating disk electrode (RDE) technique is a convenient technique to determine the kinetics and the mechanism of electrochemical electrode reactions. Linear sweep voltammetric (LSV) studies were performed on AgNPs/PAP/GCE in the presence of DMAB to determine the kinetic parameters more quantitatively (Figure 8A). Based on the RDE results at a chosen potential, the number of electrons transferred in the redox reaction can be calculated using the Koutecky–Levich (K–L) equation (5) [65] as follows.

$$\frac{1}{j} = \frac{1}{j_k} + \frac{1}{0.62\ n\ F\ A\ C_{DMAB}\ D^{\frac{2}{3}}{}_{DMAB}\ \omega^{\frac{1}{2}}\ \gamma^{\frac{-1}{6}}} \tag{5}$$

where j is the measured current density, j_k is the kinetic current density, ω is the electrode rotation rate (rad/s), n is the number of electrons transferred for DMAB, F is Faraday constant (96485) C mol^{-1}), C_{DMAB} is the concentration of DMAB in 2.0 M NaOH (5 $\times 10^{-6}$ mol cm^{-3}), D_{DMAB} is the diffusion coefficient of DMAB [13], γ is the kinematic viscosity of the solution (0.0117 cm^2 s^{-1}) which is determined with Oswald viscosimeter at 25 °C. According to the equations, the n was calculated from the slope of the Koutecky–Levich plot j^{-1} vs. $\omega^{-1/2}$ (Figure 8B). The calculated total electron number for DMAB oxidation is 5.6, which is close to the theoretical value of 6.

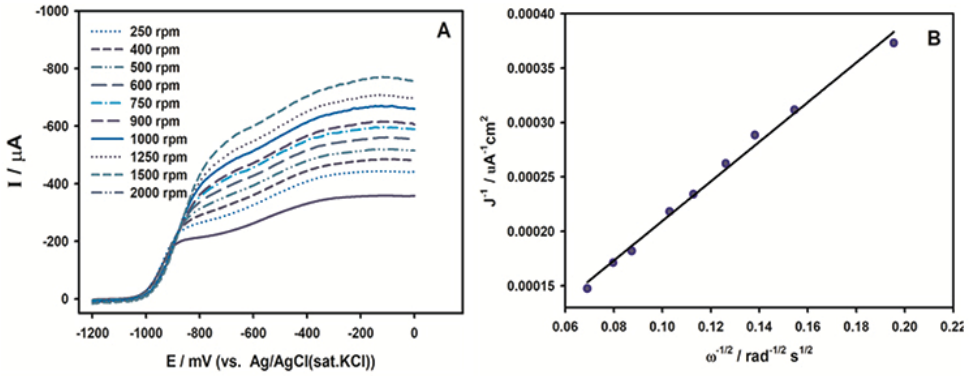

Figure 8. A) LSVs of rotating AgNPs/PAP/GCE in 2.0 M NaOH containing 5.0 mM DMAB solution at different rotation rates (250 to 2000 rpm). B) Koutecky–Levich (K-L) plot of AgNPs/PAP/GCE derived from Figure 8A.

There are a limited number of studies on DMAB oxidation in fuel cell applications. These studies are as follows; the electrochemical behavior of DMAB on Au bulk electrode was investigated by Finkelstein et al. [18]. The results of this study showed that the total number of electrons transferred during the oxidation of DMAB was found as 5.4. This value depends on potential and formation of H_2 bubble. The oxidation behavior of DMAB was studied by Rohan and Nagle using a gold microdisk in alkaline medium [13]. They exhibited that the electron number transferred in the electrooxidation reaction of DMAB varies from 3 to 6. It depends on the ratio of OH$-$ to DMAB, with H_2 evolution. An overall electron number of 6 have been determined with chronoamperometry results. Plana and Dryfe described the DMAB electrooxidation on polycrystalline gold electrodes at high pH [9]. They suggested two sequential three-electron processes on gold. At low potentials, three electrons are extracted from the molecule, denoting that hydrogen is not oxidized, whereas at high potential a six-electron oxidation occurs. In another study investigating the oxidation behavior of DMAB, Pt was used as the electrode [8]. Martins and Nunes evaluated the effect of DMAB concentration on the number of electrons transferred in the electrooxidation reaction. In the electrooxidation of DMAB on the Pt surface, the transferred

electron numbers were calculated as 3.86, 4.68, and 3.76 from the discharge curves for three different DMAB concentrations. The reason for the low number of electrons is that the platinum surface catalyzes the formation of hydrogen, causing hydrolysis of DMAB. Sadik et al. explained electron transfer mechanism for the DMAB on gold surface in KOH solution [15]. This study has highlighted the pH-dependence of DMAB oxidation on gold in alkaline solution. The total number of electrons transferred in oxidation of DMAB on gold surface was calculated using the rotating disk electrode (RDE) as 5.74. All these studies examining the oxidation mechanism of DMAB show that the number of electrons transferred in electrode reaction on all gold-based surfaces is close to the theoretical number of 6. According to the results, it can be said that DMAB has direct oxidation reaction on gold surfaces. Conversely, when the platinum surface is used as the electrode, it is found that the number of electrons is reduced due to the formation of hydrogen. In our study, the number of electrons transferred in the DMAB oxidation on AgNPs/PAP/GCE surface was found to be 5.6. Although this value is consistent with the literature, it shows that direct oxidation reaction takes place. Furthermore, compared to gold and platinum electrodes, the proposed AgNPs-PAP composite electrode is advantageous in that it is relatively inexpensive, stable, and easy to prepare.

3.5. Stability of AgNPs/PAP/GCE

Stability is a challenging issue for fuel cell applications. For this purpose, chronoamperometry was applied at AgNPs/PAP/GCE and Ag wire to test the signal change during this measurement towards the response of 8 mM DMAB (Figure 9). In both chronoamperometric curves, the currents were dropped rapidly at first and then became relatively stable. The higher steady-state peak current was achieved at AgNPs/PAP/GCE as compared to the Ag wire. Moreover, a long-term storage of the AgNPs/PAP/GCE was investigated by keeping the electrode in vapor of the 2.0 M NaOH solution when no measurement was taken. The response showed no significant change in the peak current and peak potential of DMAB after 1 month. These results prove that AgNPs/PAP/GCE is a stable and efficient surface for the oxidation of DMAB.

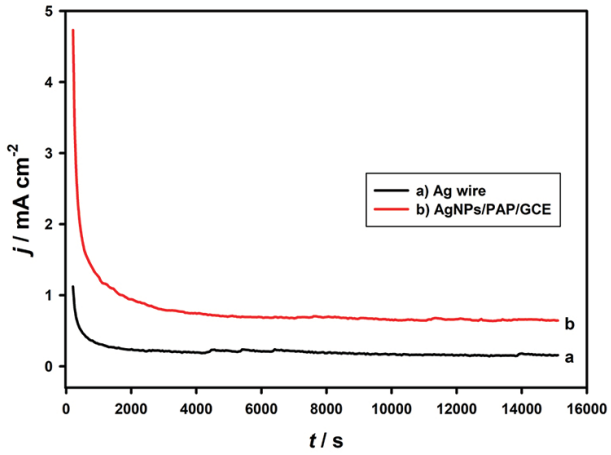

Figure 9. Stability of AgNPs/PAP/GCE and Ag wire in 2.0 M NaOH containing 8.0 mM DMAB for 15,000 s.

4. Conclusion

In the present work, AgNPs/PAP/GCE catalyst has been prepared by electrochemical synthesis of AgNPs after electrochemical formation of poly aminophenol film on glassy carbon electrode surface. Morphological

and chemical characterization of the AgNPs/PAP/GCE was carried out by SEM, TEM, EDX, XPS, and EIS techniques. The SEM images revealed that spherical AgNPs were distributed homogeneously on the PAP/GCE with the average size of approximately 100 nm. From the XPS results, it clarified that Ag species inside the PAP were chiefly dispersed as metallic Ag. Cyclic voltammograms of DMAB were indicated that higher electrocatalytic activity is obtained on the AgNPs/PAP/GCE as compared to the GCE and PAP/GCE in alkaline media. Experimental procedures such as cycle number of aminophenol polymerization, cycle number of Ag deposition, and NaOH concentration have also been optimized. The electrocatalytic oxidation of DMAB at AgNPs/PAP/GCE was found to proceed via 5.6 electron transfer, which was calculated from RDE results. It shows that direct oxidation reaction of DMAB takes place on AgNPs/PAP/GCE. The stability studies were performed by chronoamperometric technique and the results indicated that the AgNPs/PAP/GCE was introduced as a stable and efficient surface for the oxidation of DMAB. The overall results demonstrated that the AgNPs/PAP/GCE is a promising alternative as cheap, stable, and easy prepared anode material for direct DMAB fuel cells.

Acknowledgments

The Scientific and Technical Research Council of Turkey (TÜBİTAK) (project number:110T806), EBILTEM (project number: BIL-012), and Ege University Research Funds (BAP project: 12 FEN/039) supported this work.

References

1. Boudghene Stambouli A, Traversa E. Fuel cells, an alternative to standard sources of energy. Renewable and Sustainable Energy Reviews 2002; 6 (3): 295-304. doi: 10.1016/S1364-0321(01)00015-6
2. Artyushkova K, Serov A, Doan H, Danilovic N, Capuano CB et al. Application of X-ray photoelectron spectroscopy to studies of electrodes in fuel cells and electrolyzers. Journal of Electron Spectroscopy and Related Phenomena 2019; 231: 127-139. doi: 10.1016/j.elspec.2017.12.006
3. Andújar JM, Segura F. Fuel cells: History and updating. A walk along two centuries. Renewable and Sustainable Energy Reviews 2009; 13 (9): 2309-2322. doi: 10.1016/j.rser.2009.03.015
4. Liu CH, Wang HM, Lin KJ, Kuo HC, Weng YH et al. Long-term neurotoxic effects of dimethylamine borane intoxication. Journal of the Neurological Sciences 2012; 319 (1-2): 147-151. doi: 10.1016/j.jns.2012.05.013
5. Homma T, Tamaki A, Nakai H, Osaka T. Molecular orbital study on the reaction process of dimethylamine borane as a reductant for electroless deposition. Journal of Electroanalytical Chemistry 2003; 559: 131-136. doi: 10.1016/S0022-0728(03)00042-1
6. Wojnicki M, Rudnik E, Luty-Błocho M, Pacławski K, Fitzner K. Kinetic studies of gold(III) chloride complex reduction and solid phase precipitation in acidic aqueous system using dimethylamine borane as reducing agent. Hydrometallurgy 2012; 127-128: 43-53. doi: 10.1016/j.hydromet.2012.06.015
7. Vaškelis A, Tarozaite R, Jagminiene A, Tamašiunaite LT, Juškenas R et al. Gold nanoparticles obtained by Au(III) reduction with Sn(II): Preparation and electrocatalytic properties in oxidation of reducing agents. Electrochimica Acta 2007; 53 (2): 407-416. doi: 10.1016/j.electacta.2007.04.008
8. Martins JI, Nunes MC. Comparison of the electrochemical oxidation of borohydride and dimethylamine borane on platinum electrodes: Implication for direct fuel cells. Journal of Power Sources 2008; 175 (1): 244-249. doi: 10.1016/j.jpowsour.2007.09.028

9. Plana D, Dryfe RAW. The electro-oxidation of dimethylamine borane: Part 1, polycrystalline substrates. Electrochimica Acta 2011; 56 (11): 3835-3844. doi: 10.1016/j.electacta.2011.02.041

10. Bayatsarmadi B, Peters A, Talemi P. Catalytic polymeric electrodes for direct borohydride fuel cells. Journal of Power Sources 2016; 322: 26-30. doi: 10.1016/j.jpowsour.2016.04.137

11. Celik C, Boyaci San FG, Sarac HI. Effects of operation conditions on direct borohydride fuel cell performance. Journal of Power Sources 2008; 185 (1): 197-201. doi: 10.1016/j.jpowsour.2008.06.066

12. Pylypko S, Zadick A, Chatenet M, Miele P, Cretin M et al. A preliminary study of sodium octahydrotriborate NaB_3H_8 as potential anodic fuel of direct liquid fuel cell. Journal of Power Sources 2015; 286: 10-17. doi: 10.1016/j.jpowsour.2015.03.143

13. Nagle LC, Rohan JF. Investigation of DMAB Oxidation at a Gold Microelectrode in Base. Electrochemical and Solid-State Letters 2005; 8 (5): C77-C80. doi: 10.1149/1.1883905

14. Plana D, Rodriguez P, Koper MTM, Dryfe RAW. The electro-oxidation of dimethylamine borane: Part 2, in situ FTIR on single-crystal gold electrodes. Electrochimica Acta 2011; 56 (22): 7637-7643. doi: 10.1016/j.electacta.2011.06.072

15. Sadik OA, Xu H, Sargent A. Multi-electron transfer mechanism of dimethylamine borane in electroless gold deposition. ournal of Electroanalytical Chemistry 2005; 583 (2): 167-175. doi: 10.1016/j.jelechem.2005.05.013

16. Burke LD, Lee BH. Oxidation of some reducing agents used in electroless plating baths at gold anodes in aqueous media. Journal of Applied Electrochemistry 1992; 22 (1): 48-56. doi: 10.1007/BF01093011

17. Sargent A, Sadik OA. Probing the mechanism of electroless gold plating using an EQCM II. Effect of Bath Additives on Interfacial Plating Processes. Journal of Electrochemical Society 2001; 148 (6): 413-420. doi: 10.1149/1.1370963

18. Finkelstein DA, Da Mota N, Cohen JL, Abruña HD. Rotating disk electrode (RDE) investigation of BH_4^- and BH_3OH^- electro-oxidation at Pt and Au: Implications for BH_4^- fuel cells. The Journal of Physical Chemistry C 2009; 113 (45): 19700-19712. doi: 10.1021/jp900933c

19. Vijwani H, Mukhopadhyay SM. Palladium nanoparticles on hierarchical carbon surfaces: A new architecture for robust nano-catalysts. Applied Surface Science 2012; 263: 712-721. doi: 10.1016/j.apsusc.2012.09.146

20. Hua M, Zhang S, Pan B, Zhang W, Lv L et al. Heavy metal removal from water/wastewater by nanosized metal oxides: A review. Journal of Hazardous Materials 2012; 211-212: 317-331. doi: 10.1016/j.jhazmat.2011.10.016

21. Solanki JN, Murthy ZVP. Highly monodisperse and sub-nano silver particles synthesis via microemulsion technique. Colloids and Surfaces A: Physicochemical and Engineering Aspects 2010; 359 (1-3): 31-38. doi: 10.1016/j.colsurfa.2010.01.058

22. Lecerf N, Mathur S, Shen H, Veith M, Hüfner S. Chemical vapour and SOL-GEL syntheses of nano-composites and ceramics using metal-organic precursors. Scripta Materialia 2001; 44 (8-9): 2157-2160. doi: 10.1016/S1359-6462(01)00913-7

23. Lee DW, Kim BK. Synthesis of nano-structured titanium carbide by Mg-thermal reduction. Scripta Materialia 2003; 48 (11): 1513-1518. doi: 10.1016/S1359-6462(03)00130-1

24. Driess M, Merz K, Schoenen R, Rabe S, Kruis FE et al. From molecules to metastable solids: Solid-state and chemical vapour syntheses (CVS) of nanocrystalline ZnO and Zn. Comptes Rendus Chimie 2003; 6 (3): 273-281. doi: 10.1016/S1631-0748(03)00040-7

25. Kim K Do, Han DN, Kim HT. Optimization of experimental conditions based on the Taguchi robust design for the formation of nano-sized silver particles by chemical reduction method. Chemical Engineering Journal 2004; 104 (1-3): 55-61. doi: 10.1016/j.cej.2004.08.003

26. Liguo Y, Yanhua Z. Preparation of nano-silver flake by chemical reduction method. Rare Metal Materials and Engineering 2010; 39 (3): 401-404. doi: 10.1016/s1875-5372(10)60088-4

27. Habibi B, Pournaghi-Azar MH. Methanol oxidation on the polymer coated and polymer-stabilized Pt nanoparticles: A comparative study of permeability and catalyst particle distribution ability of the PANI and its derivatives. International Journal of Hydrogen Energy 2010; 35 (17): 9318-9328. doi: 10.1016/j.ijhydene.2010.01.088

28. Arslan E, Çakir S. Electrochemical fabrication of polyproline modified graphite electrode decorated with Pd-Au bimetallic nanoparticles: Application for determination of carminic acid. Journal of Electroanalytical Chemistry 2016; 760: 32-41. doi: 10.1016/j.jelechem.2015.11.042

29. Shahrokhian S, Salimian R, Rastgar S. Pd-Au nanoparticle decorated carbon nanotube as a sensing layer on the surface of glassy carbon electrode for electrochemical determination of ceftazidime. Materials Science and Engineering C 2014; 34 (1): 318-325. doi: 10.1016/j.msec.2013.09.014

30. El-Nagar GA, El-Deab MS, Mohammad AM, El-Anadouli BE. Promoting effect of hydrocarbon impurities on the electro-oxidation of formic acid at Pt nanoparticles modified GC electrodes. Electrochimica Acta 2015; 180: 268-279. doi: 10.1016/j.electacta.2015.08.119

31. Ensafi AA, Abarghoui MM, Rezaei B. Simultaneous determination of morphine and codeine using Pt nanoparticles supported on porous silicon flour modified ionic liquid carbon paste electrode. Sensors and Actuators B Chemical 2015; 219: 1-9. doi: 10.1016/j.snb.2015.05.010

32. Shahrokhian S, Hafezi-Kahnamouei M. Glassy carbon electrode modified with a nanocomposite of multi-walled carbon nanotube decorated with Ag nanoparticles for electrochemical investigation of Isoxsuprine. Journal of Electroanalytical Chemistry 2018; 825: 30-39. doi: 10.1016/j.jelechem.2018.08.010

33. Asadian E, Iraji Zad A, Shahrokhian S. Voltammetric studies of Azathioprine on the surface of graphite electrode modified with graphene nanosheets decorated with Ag nanoparticles. Materials Science and Engineering C 2016; 58: 1098-1104. doi: 10.1016/j.msec.2015.09.022

34. Shahrokhian S, Ranjbar S, Ghalkhani M. Modification of the Electrode Surface by Ag Nanoparticles Decorated Nano Diamond-graphite for Voltammetric Determination of Ceftizoxime. Electroanalysis 2016; 28 (3): 469-476. doi: 10.1002/elan.201500377

35. Cui K, Song Y, Yao Y, Huang Z, Wang L. A novel hydrogen peroxide sensor based on Ag nanoparticles electrodeposited on DNA-networks modified glassy carbon electrode. Electrochemistry Communications 2008; 10 (4): 663-667. doi: 10.1016/j.elecom.2008.02.016

36. Kavian S, Azizi SN, Ghasemi S. Electrocatalytic detection of hydrazine on synthesized nanozeolite-supported Ag nanoparticle-modified carbon paste electrode at a negative potential in an alkaline medium. Journal of Molecular Liquids 2016; 218: 663-669. doi: 10.1016/j.molliq.2016.02.090

37. Porras-Gutiérrez AG, Frontana-Uribe BA, Gutiérrez-Granados S, Griveau S, Bedioui F. In situ characterization by cyclic voltammetry and conductance of composites based on polypyrrole, multi-walled carbon nanotubes and cobalt phthalocyanine. Electrochimica Acta 2013; 89: 840-847. doi: 10.1016/j.electacta.2012.11.018

38. Guimard NK, Gomez N, Schmidt CE. Conducting polymers in biomedical engineering. Progress in Polymer Science 2007; 32 (8-9): 876-921. doi: 10.1016/j.progpolymsci.2007.05.012

39. Kuilla T, Bhadra S, Yao D, Kim NH, Bose S, Lee JH. Recent advances in graphene based polymer composites. Progress in Polymer Science 2010; 35 (11): 1350-1375. doi: 10.1016/j.progpolymsci.2010.07.005

40. Ciszewski A, Milczarek G. Electrochemical detection of nitric oxide using polymer modified electrodes. Talanta 2003; 61 (1): 11-26. doi: 10.1016/S0039-9140(03)00355-2

41. Ensafi AA, Amini M. A highly selective optical sensor for catalytic determination of ultra-trace amounts of nitrite in water and foods based on brilliant cresyl blue as a sensing reagent. Sensors and Actuators B: Chemical 2010; 147 (1): 61-66. doi: 10.1016/j.snb.2010.03.014

42. Kuwahara T, Ohta H, Kondo M, Shimomura M. Immobilization of glucose oxidase on carbon paper electrodes modified with conducting polymer and its application to a glucose fuel cell. Bioelectrochemistry 2008; 74 (1): 66-72. doi: 10.1016/j.bioelechem.2008.07.002

43. Wang Z, Gao G, Zhu H, Sun Z, Liu H et al. Electrodeposition of platinum microparticle interface on conducting polymer film modified nichrome for electrocatalytic oxidation of methanol. International Journal of Hydrogen Energy 2009; 34 (23): 9334-9340. doi: 10.1016/j.ijhydene.2009.09.062

44. Ehsani A, Mahjani MG, Jafarian M, Naeemy A. Electrosynthesis of polypyrrole composite film and electrocatalytic oxidation of ethanol. Electrochimica Acta 2012; 71: 128-133. doi: 10.1016/j.electacta.2012.03.107

45. Koçak ÇC, Dursun Z. Simultaneous determination of ascorbic acid, epinephrine and uric acid at over-oxidized poly(p-aminophenol) film modified electrode. Journal of Electroanalytical Chemistry 2013; 694: 94-103. doi: 10.1016/j.jelechem.2013.02.006

46. Karabiberoğlu ŞU, Dursun Z. Highly catalytic activity of platinum-gold particles modified poly(p-aminophenol) electrode for oxygen reduction reaction. Journal of Solid State Electrochemistry 2016; 20 (7): 2009-2018. doi: 10.1007/s10008-016-3201-z

47. Karabiberoğlu ŞU, Koçak ÇC, Koçak S, Dursun Z. Polymer Film Supported Bimetallic Au–Ag Catalysts for Electrocatalytic Oxidation of Ammonia Borane in Alkaline Media. Nano-Micro Letters 2016; 8 (4): 358-370. doi: 10.1007/s40820-016-0095-3

48. Karabiberoğlu ŞU, Dursun Z. Over-Oxidized Poly (Phenol Red) Film Modified Glassy Carbon Electrode for Anodic Stripping Voltammetric Determination of Ultra-Trace Antimony (III). Electroanalysis 2017; 29 (4): 1069-1080. doi: 10.1002/elan.201600629

49. Mu S. Direct determination of arsenate based on its electrocatalytic reduction at the poly(aniline-co-o-aminophenol) electrode. Electrochemistry Communications 2009; 11 (7): 1519-1522. doi: 10.1016/j.elecom.2009.05.050

50. Barbero C, Silber JJ, Sereno L. Electrochemical properties of poly-ortho-aminophenol modified electrodes in aqueous acid solutions. Journal of Electroanalytical Chemistry 1990; 291 (1-2): 81-101. doi: 10.1016/0022-0728(90)87179-N

51. Menon S, Jesny S, Girish Kumar K. A voltammetric sensor for acetaminophen based on electropolymerized-molecularly imprinted poly(o-aminophenol) modified gold electrode. Talanta 2018; 179: 668-675. doi: 10.1016/j.talanta.2017.11.074

52. Valdés García MA, Tuñón Blanco P, Ivaska A. A poly(o-aminophenol) modified electrode as an amperometric hydrogen peroxide biosensor. Electrochimica Acta 1998; 43 (23): 3533-3539. doi: 10.1016/S0013-4686(98)00101-7

53. Pishahang J, Amiri HB, Heli H. Synthesis of carbon nanoparticles-poly(ortho-aminophenol) nanocomposite and its application for electroanalysis of iodate. Sensors and Actuators B Chemical 2018; 256: 878-887. doi: 10.1016/j.snb.2017.10.030

54. Koçak ÇC, Nas A, Kantekin H, Dursun Z. Simultaneous determination of theophylline and caffeine on novel [Tetra-(5-chloroquinolin-8-yloxy) phthalocyanato] manganese(III)-Carbon nanotubes composite electrode. Talanta 2018; 184: 452-460. doi: 10.1016/j.talanta.2018.03.029

55. Tucceri R. Effect of prolonged electrode potential cycling on the charge transport parameters of poly(o-aminophenol) films. A study employing rotating disc electrode voltammetry and surface resistance. Journal of Electroanalytical Chemistry 2014; 717-718: 131-139. doi: 10.1016/j.jelechem.2014.01.023

56. Wang C, Xiong Z, Sun P, Wang R, Zhao X et al. Facile longitudinal unzipped multiwalled carbon nanotubes incorporated overoxidized poly(p-aminophenol) modified electrode for sensitive simultaneous determination of dopamine, uric acid and tryptophan. Journal of Electroanalytical Chemistry 2017; 801: 395-402. doi:10.1016/j.jelechem.2017.08.028

57. Liu L-P, Yin Z-J, Yang Z-S. A l-cysteine sensor based on Pt nanoparticles/poly(o-aminophenol) film on glassy carbon electrode. Bioelectrochemistry 2010; 79 (1): 84-89. doi: 10.1016/J.BIOELECHEM.2009.12.003

58. Carbone ME, Ciriello R, Guerrieri A, Salvi AM. Poly(o-aminophenol) electrosynthesized onto platinum at acidic and neutral ph: Comparative investigation on the polymers characteristics and on their inner and outer interfaces. Internatinal Journal of Electrochemical Science 2014; 9 (4): 2047-2066.

59. Carbone ME, Ciriello R, Granafei S, Guerrieri A, Salvi AM. EQCM and XPS investigations on the redox switching of conducting poly(o-aminophenol) films electrosynthesized onto Pt substrates. Electrochimica Acta 2015; 176: 926-940. doi: 10.1016/j.electacta.2015.07.047

60. Carbone ME, Ciriello R, Granafei S, Guerrieri A, Salvi AM. Electrosynthesis of conducting poly(o-aminophenol) films on Pt substrates: A combined electrochemical and XPS investigation. Electrochimica Acta 2014; 144: 174-185. doi: 10.1016/j.electacta.2014.08.047

61. Kong FY, Yao L, Li RF et al. Synthesis of nitrogen-doped reduced graphene oxide loading with Au-Ag bimetallic nanoparticles for electrochemical detection of daunorubicin. Journal of Alloys and Compounds 2019; 797: 413-420. doi: 10.1016/j.jallcom.2019.04.276

62. Rahman MM, Wahid A, Alam MM, Asiri AM. Efficient 4-Nitrophenol sensor development based on facile $Ag@Nd_2O_3$ nanoparticles. Materials Today Communications 2018; 16: 307-313. doi: 10.1016/j.mtcomm.2018.07.009

63. Prasad KS, Chuang M, Ho JA. Synthesis, characterization, and electrochemical applications of carbon nanoparticles derived from castor oil soot. Talanta 2012; 88: 445-449. doi: 10.1016/j.talanta.2011.10.056

64. Carvalho RC, Gouveia-Caridade C, Brett CMA. Glassy carbon electrodes modified by multiwalled carbon nanotubes and poly(neutral red): A comparative study of different brands and application to electrocatalytic ascorbate determination. Analytical and Bioanalytical Chemistry 2010; 398 (4): 1675-1685. doi: 10.1007/s00216-010-3966-3

65. Araminait R, Garjonyt R, Malinauskas A. Rotating disk electrode study of Prussian blue- and glucose oxidase-based bioelectrode. Journal of Electroanalalytical Chemistry 2012; 672: 12-16. doi: 10.1016/j.jelechem.2012.03.005